The Protective Effect of *Trichilia catigua* A. Juss. on DEHP-Induced Reproductive System Damage in Male Mice

Xinyue Chang, Mingran Dong, Xiao Mi, Meigeng Hu, Juan Lu* and Xi Chen*

Institute of Medicinal Plant Development, Chinese Academy of Medical Sciences, Peking Union Medical College, Beijing, China

The present study aimed to explore the protective effect and molecular mechanisms of *Trichilia catigua* A. Juss. extract (TCE) against di (2-ethylhexyl) phthalate (DEHP)-induced damage to the reproductive system of mice. Acute toxicity tests revealed that the maximum tolerated dose (MTD) in mice was up to $2.7 \, g \, kg^{-1}$. After induction with DEHP, TCE (L-TCE, M-TCE, H-TCE) was orally administered to mice for 28 days. Differences in indicators among groups showed that TCE significantly improved the anogenital distance and the organ indexes of the epididymides and testes. It also significantly reduced varicocele and interstitial cell lesions compared to the model group. H-TCE reduced the sperm abnormality rate, increased the levels of sex hormones, Na^+K^+ and Mg^{2+}, Ca^{2+}-ATPase enzyme activity, antioxidant enzyme vitality, coupled with a significant decrease in LH and MDA contents. The levels of testicular marker enzymes ACP and LDH were significantly augmented by both M-TCE and H-TCE. Further studies claimed that DEHP induction reduced the mRNA expression levels of *Nrf2, SOD2, SOD3, CDC25C CDK1, CYP11A1, 3β-HSD, 5α-R, AR, SF1,* and *CYP17A1,* increased the level of *Keap1,* while TCE reversed the expression levels of these genes. Meanwhile, IHC results demonstrated a significant change in the expression activity of the relevant proteins compared to the control group. The results suggest that M-TCE and H-TCE enabled the recovery of DEHP-induced reproductive system damage in male mice by improving testicular histopathology, repairing testicular function, and reducing oxidative stress damage. The oxidation-related Keap1-Nrf2 pathway, SODs enzyme, the cell cycle control-related CDC25C-CDK1 pathway, and the steroidogenic-related pathway may contribute to this protective effects of TCE.

Keywords: *Trichilia catigua*, DEHP, phenolic, reproductive system, oxidative damage

---

Abbreviations: ACP, acid phosphatase; AKP, alkaline phosphatase; BTB, blood-testis barrier; CAT, catalase; DEHP, di-(2-ethylhexyl) phthalate; E2, estradiol; FSH, follicle-stimulating hormone; GR, glutathione reductases; GSH, reduced glutathione; GSH-Px, glutathione peroxidase; i.g., intragastric administration; IHC, immunochemical; LD0, 0% lethal dose; LD50, median lethal dose; LD100, 100% lethal dose; LDH, lactate dehydrogenase; LH, luteinizing hormone; MDA, malondialdehyde; MTD, maximum tolerated dose; SOD, superoxide dismutase; T, testosterone; TCE, *Trichilia catigua* A. Juss. extract; qRT-PCR, quantitative real-time PCR.

GRAPHICAL ABSTRACT |
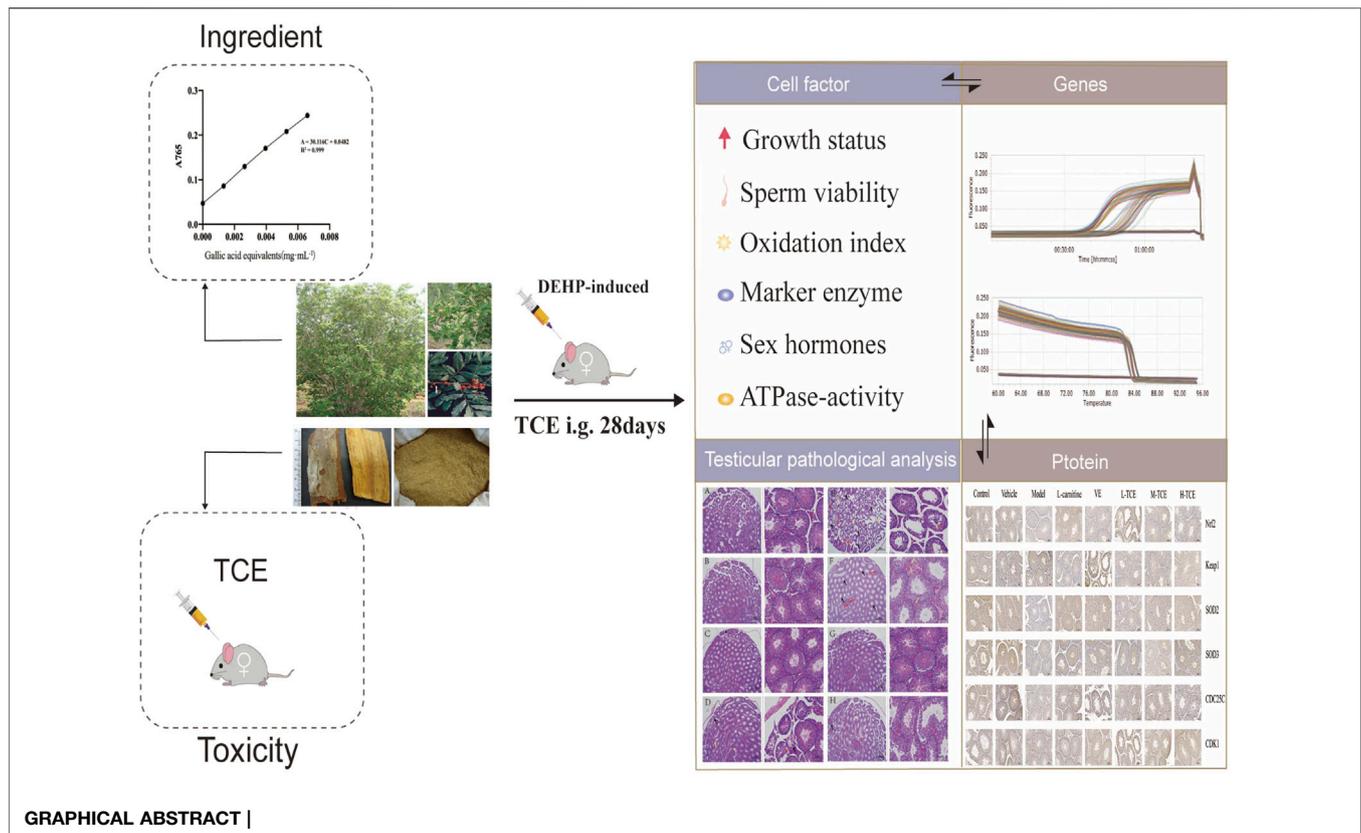
INTRODUCTION

Several predisposing factors that are responsible for the decline in sperm quality and count have been reported in the past 50 years (Damstra et al., 2002; Merzenich et al., 2010). Primarily, environmental triggers and lifestyle, including endocrine-disrupting chemicals, can significantly impact male reproductive health (Street et al., 2018). One of the most widely used plasticizers, di (2-ethylhexyl) phthalate (DEHP), can enter the body through drinking, eating, skin contact (cosmetics), and breathing. The estrogen-like effects of DEHP affect the normal secretion of hormones in living organisms, causing varying degrees of harm to human health (Farombi et al., 2007; Muczynski et al., 2012). Studies have reported that DEHP interferes with the reproductive endocrine system, reducing sperm motility, decreasing sperm count, causing atrophy and morphological abnormalities in parenchymal organs such as the testis, and is thus highly toxic to the male reproductive system (Saunders et al., 1997; Lyche et al., 2009; Abd-Ellah et al., 2016). The pathophysiological mechanism behind phthalate-induced atrophy in several tissues may be attributed to oxidative stress (Farombi et al., 2007; Muczynski et al., 2012). These are involved in deregulation in the balance of antioxidant defense in tissues and induction of peroxidative damage (Andrade et al., 2006). Several studies have documented that oxidative damage induced by phthalates can lead to DNA damage and impaired mitochondrial function, reducing the activity of genes associated with high pass synthesis, impeding organ development and testicular sperm production (Yeung et al., 2011; Barakat et al., 2017; Barakat et al., 2019).

Trichilia catigua A. Juss. is a small shrubby tree prevalent in South America. It is commonly used locally in Brazil as an aphrodisiac tonic. Preparations of this herb also find application in folk medicine to alleviate fatigue, stress, and improve memory. Recent research has confirmed several pharmacological activities, including antioxidant, antinociceptive, anti-inflammatory, and neuroprotective effects of *Trichilia catigua* (Silva, 2004; Longhini et al., 2017). Alcoholic extract of the *Trichilia catigua* bark, traditionally known as "Catuama" (Pizzolatti et al., 2002), exhibits significant effects in stimulating erection time in the rabbit cavernosa and is generally exploited as a stimulant of the reproductive system and as an anti-fatigue drug (Antunes et al., 2001; Silva, 2004). Available studies indicate the safety of *Trichilia catigua* for use in healthy human volunteers, with no known side effects or adverse effects (Oliveira et al., 2005). The presence of several secondary metabolites, including omega-phenyl alkanes, omega-phenyl alkanoic acids, omega-phenyl-gamma-lactones, alkyl-gamma-lactones, alkenyl-gamma-lactones, fatty acids, b-sitosterol, stigmasterol, campesterol, epicatechin, cinchonains (Ia, Ib, IIa, IIb), catiguanins A and B, procyanidins B2 and C1, tannins, and a mixture of flavalignans, has been reported by phytochemical studies on *Trichilia catigua* (Tang et al., 2007).

TABLE 1 | Primers for real-time PCR analyses.

Gene	Species	Forward (5′-3′)	Reverse (3′-5′)
GAPDH	Mouse	AGGTCGGTGTGAACGGATTTG	TGTAGACCATGTAGTTGAGGTCA
Nrf2	Mouse	TAGATGACCATGAGTCGCTTGC	GCCAAACTTGCTCCATGTCC
H O -1	Mouse	GATAGAGCGCAACAAGCAGAA	CAGTGAGGCCCATACCAGAAG
Keap1	Mouse	TCGAAGGCATCCACCCTAAG	CTCGAACCACGCTGTCAATCT
INOS	Mouse	GTTCTCAGCCCAACAATACAAGA	GTGGACGGGTCGATGTCAC
SOD1	Mouse	AACCAGTTGTGTTGTCAGGAC	CCACCATGTTTCTTAGAGTGAGG
SOD2	Mouse	CAGACCTGCCTTACGACTATGG	CTCGGTGGCGTTGAGATTGTT
SOD3	Mouse	CCTTCTTGTTCTACGGCTTGC	TCGCCTATCTTCTCAACCAGG
CAT	Mouse	TGGCACACTTTGACAGAGAGC	CCTTTGCCTTGGAGTATCTGG
PGC1α	Mouse	TATGGAGTGACATAGAGTGTGCT	GTCGCTACACCACTTCAATCC
CDC25A	Mouse	TTTTGGACAGTGACCCAAGAGA	TCTTTAATGAGACCGGCAAACTT
CDC25C	Mouse	GTTTCAGCACCCAGTTTTAGGT	AGAATGCTTAGGTTTGCCGAG
CDK1	Mouse	AAATCCTCCAGGGAATTGTGTTT	CAGCCAGTTTGATTGTTCCTTTG
Wee1	Mouse	TTCCGGCTCTGTTAAACTCCG	CGACACCGTCCTGAGGAATG
star	Mouse	AACGGGGACGAAGTGCTAAG	CCGTGTCTTTTCCAATCCTCTG
P450scc	Mouse	AGGTCCTTCAATGAGATCCCTT	TCCCTGTAAATGGGGCCATAC
CYP11A1	Mouse	AGGTCCTTCAATGAGATCCCTT	TCCCTGTAAATGGGGCCATAC
CYP17A1	Mouse	GTCGCCTTTGCGGATAGTAGT	TGAGTTGGCTTCCTGACATATCA
3β-HSD	Mouse	GGCAAATTCTCCATAGCCAA	GCTTCCTCCCAGTTGACAAG
5α-R	Mouse	GAGTTGGATGAGTTGCGCCTA	GGACCACTGCGAGGAGTAG
AR	Mouse	CAGGAGGTAATCTCCGAAGGC	ACAGACACTGCTTTACACAACTC
SP1	Mouse	AGGGTCCGAGTCAGTCAGG	CTCGCTGCCATTGGTACTGTT
SF1	Mouse	GAGAGTTCCGTACCCGCAAAA	CTCTGGGTCCAATTAGGAGCC
Occludin	Mouse	TGAAAGTCCACCTCCTTACAGA	CCGGATAAAAAGAGTACGCTGG
Z O -1	Mouse	GCTTTAGCGAACAGAAGGAGC	TTCATTTTTCCGAGACTTCACCA

TABLE 2 | Secondary antibody information and dilutions.

Name	Brand	Specie	Batch No.	Dilution
Anti-KEAP1 antibody	Bioss	Rabbit	bs-3648R	1:400
Anti-Nrf2antibody	Bioss	Rabbit	bs-1074R	1:400
Anti-CDC25C antibody	Bioss	Rabbit	bs-9597R	1:200
Anti-SOD2 antibody	Bioss	Rabbit	bs-20667R	1:300
Anti-SOD3 antibody	Bioss	Rabbit	bs-3895R	1:300
Anti-CDK1 antibody	Bioss	Rabbit	bs-1341R	1:300

Trichilia catigua finds widespread application in folk medicine to treat free radical-related diseases. Modern pharmacological research has attempted to determine its antioxidant activity in a neurological context. Nonetheless, there is little information in the literature about *Trichilia catigua's* antioxidant properties on the reproductive system. We, therefore, employed DEHP to construct a model of reproductive system oxidative stress damage to investigate the reproductive system antioxidant damage activity of ethanol extracts from the stem and bark of *Trichilia catigua*.

MATERIALS AND METHODS

Equipment and Reagents

The equipment used for this study was as follows: AB265-S Analytical Balance (METTLER TOLEDO, Switzerland), BCD-206TS Haier Refrigerator (Qingdao Haier Co., Ltd.), DZKW-4 Electronic Thermostatic Water Bath [Linmao Technology (Beijing) Co., Ltd.], FJ-200 High-Speed Dispersion Homogenizer (Shanghai Specimen Model Factory), NanoDrop 2000 Spectrophotometers (Thermo Fisher Scientific Inc., MA, United States), LightCycler® 480 Real-Time System (Roche, United States), Biological microscopes (Nikon, eclipse Ci., Japan), MDF-U53V ultra-low temperature refrigerator (SANYO, Japan).

The following reagents were employed in the present study: *Trichilia catigua* A. Juss. was provided by FITOTERAPIA BIOTECH LTDA, collected in Bahia, Northeast Brazil, was identified by Li Haitao, Yunnan Branch, Institute of Medicinal Plants, Chinese Academy of Medical Sciences. Folin-Phenol (F8060, Solarbio). Gallic acid (151017) was purchased from Shanghai Winherb Medical Technology Co., Ltd. (Shanghai, China). The purity of standards chemicals ≥98%. DEHP (Alfa Aesar, A10415), Superoxide dismutase (SOD) Activity Assay (A001), Malondialdehyde (MDA) kit (A003), Catalase (CAT) assay kit (A007), Reduced glutathione (GSH) assay kit (A006), Glutathion reductases (GR) assay kit (A062), Glutathione peroxidase (GSH-Px) kit (A005), Succinate dehydrogenase (SDH) kit (A022), Acid phosphatase (ACP) assay kit (A060), Lactate dehydrogenase (LDH) kit (A020), Alkaline phosphatase (ALP/AKP) assay kit (A059) were all purchased from Nanjing Jiancheng Technology Co., Ltd. (Nanjing, China). Mlbio Mouse follicle-stimulating hormone (FSH) ELISA Kit (ml001910), Mlbio Mouse estradiol (E2) ELISA Kit (ml001962), Mlbio Mouse testosterone (T) ELISA Kit (ml001948), and Mlbio Mouse luteinizing hormone (LH) ELISA Kit (ml001948) were bought from Shanghai enzyme-linked Biotechnology Co., Ltd. (Shanghai, China). RNAiso Plus (TaKaRa Bio, Lot No. 9108–9109); Prime Script RT Master Mix (TaKaRa Bio, Lot No. DRR036A); TB Green Premix Ex Taq (TaKaRa Bio, Lot No. RR820WR).

FIGURE 1 | Standard curve of gallic acid.
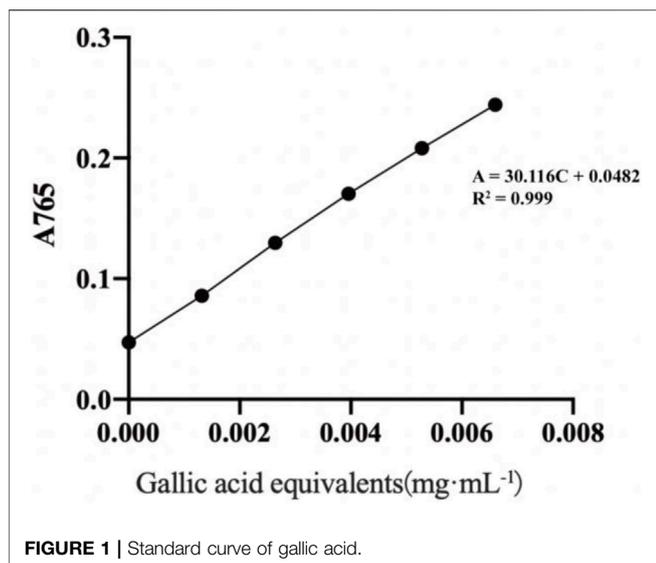
Animal

Male ICR mice (18–22 g) were obtained from Beijing HFK Bioscience Co., Ltd. (Beijing, China). The research animal ethics committee of the Institute of Medicinal Plant Development affiliated with the Chinese Academy of Medical Sciences (Beijing, China) approved all animal-related protocols

that were performed according to the National Institutes of Health guide. Animals were kept in a semi-barrier system at room temperature and humidity with a 12–12 h/light-dark photoperiod. All mice were acclimatized to the environment for 1 week before experimentation. The experimental protocol was approved by the institutional ethics committee (approval no. SLXD-20201225042 and SLXD-20210507012).

Plant Material and Extract Preparation

As per previous studies, the bark of *Trichilia catigua* was roughly extracted with water (Bernardo et al., 2018; Panizzon et al., 2019), 50% (Barbosa et al., 2004), 70% (Kamdem et al., 2012), and 95% (Pizzolatti et al., 2002) ethanol solutions to obtain four crude extracts, respectively. Subsequent extraction of these alcoholic extracts with petroleum ether, ethyl acetate, and n-butanol retrieved the corresponding nine organic phase components for a total of 13 extracts. The cell viability and the degree of oxidation of TM_4 cells damaged by H_2O_2 were compared. The results showed that the ethyl acetate fraction of the 50% alcoholic extract provided adequate protection against oxidative damage to germ cells. Therefore, we selected this component for our study.

The preparation process was as follows: 1,000 ml of 50% ethanol solution was added to 100 g of *Trichilia catigua* bark powder with the ratio of material to liquid = 1:10, thoroughly stirred, followed by cold macerate twice, each time for 24 h, and filtration. The two extracts were then combined, concentrated,

FIGURE 2 | Changes in body weight, anal anogenital distance, epididymides and testicular organ index in different groups **(A)**. Weight; **(B)**. Anogenital distance; **(C)**. Epididymides organ index; **(D)**. Testicular organ index; Means ± SD, $n = 12$; *$p < .05$, compared with the model group; **$p < .01$, compared with the model group; ##$p < .05$, compared with the control group; Control: distilled water group; Vehicle: corn oil group; Model: DEHP group; L-carnitine, VE: positive drugs group; L-TCE, M-TCE, H-TCE: low-/middle-/high-dose groups of TCE.

FIGURE 3 | Changes in the testicular pathological analysis in different groups **(A)**. Control group; **(B)**. Vehicle group; **(C)**. L-carnitine group; **(D)**. VE group; **(E)**. Model group; **(F)**. L-TCE group; **(G)**. M-TCE groups; **(H)**. H-TCE groups(x40,x200).

and dried to obtain the crude extract. The crude extract was shaken with 300 ml of distilled water to disperse it evenly in the aqueous solution, extracted with petroleum ether and ethyl acetate in turn, collected to obtain the corresponding ethyl acetate fraction, and after that spin-dried again to obtain TCE. After repeated extraction, the calculated yield of TCE powder was about 4.21%

Estimation of Total Phenolic Content
Preparation of Sample Solution
To prepare the control stock solution, 2.50 mg of gallic acid was weighed in a 25 ml volumetric flask, and the stock solution was fixed with distilled water to the scale.

Similarly, the TCE stock solution was prepared by weighing 25.00 mg of TCE in a 25 ml volumetric flask, and the stock solution was fixed with distilled water to the scale.

Establishment of the Gallic Acid Standard Curve
The total phenolic content was determined by employing the methods given in the literature (Slinkard and Singleton, 1977) with some modification. Varied amount of the control stock solution (0, 0.25, 0.5, 0.75, 1.0, 1.25 ml) was pipetted into a 25 ml volumetric flask and 1.5 ml of forintanol reagent was added. After 8 min, 1.5 ml of 10% Na_2CO_3 solution was added to the mixture, and the reaction was carried out at 25°C for 1 h. The absorbance was recorded at 765 nm. The linear regression
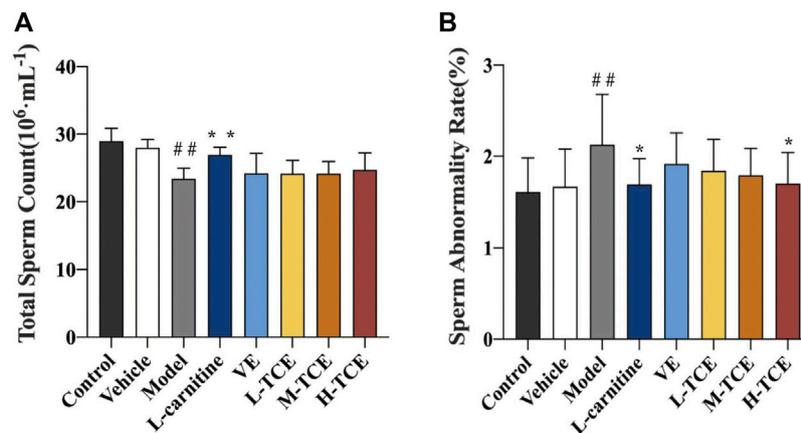
FIGURE 4 | Changes in total sperm count and sperm abnormality rates in the different groups **(A)**. Total sperm count; **(B)**. Sperm abnormality rate; Means ± SD, n = 12; *p < .05, compared with the model group; **p < .01, compared with the model group; ##p < .05, compared with the control group.

TABLE 3 | Linear equation for the determination of sex hormone content.

	Linear equations	R^2	Linear range
T	y = 0.0572x + 0.1282	0.9944	0.75–24 (ng·mL⁻¹)
LH	y = 0.0163x + 0.1089	0.9981	1.25–20 (mU·mL⁻¹)
FSH	y = 0.0104x + 0.042	0.9905	2.5–80 (mU·mL⁻¹)
E2	y = 0.0048x + 0.0017	0.9907	7.8–400 (pmol·L⁻¹)

equation was obtained with A as absorbance and C as gallic acid concentration.

Estimation of Total Phenolic Content
Following the method under 2.4.2, 1.5 ml from the sample stock solution was taken in a 25 ml volumetric flask and the absorbance was determined at 765 nm. The absorbance was repeated three times. With the help of the standard curve, the absorbance values were then employed to calculate the total polyphenol content of the sample.

Acute Toxicity Test in Mice
Corn oil was used as a co-solvent to configure a 900 mg kg⁻¹ TCE solution and diluted step by step to prepare a diluted sample solution of the appropriate concentration. Thirty-six male ICR mice (18–22 g) were randomly and evenly distributed into six groups (n = 6), including control [distilled water, intragastric administration (i.g.)] and different dosed groups (178 mg kg⁻¹, 267 mg kg⁻¹, 400 mg kg⁻¹, 600 mg kg⁻¹, 900 mg kg⁻¹ TCE, i.g.). Animals were treated for 7 days.

The mice were scrutinized for appearance, behavior, secretions, excretions, and mortality; LD50 was determined by mortality. If the LD50 value cannot be measured, dosing at 900 mg kg⁻¹ was repeated, and the MTD value was determined.

In vivo Experiments
Animal Grouping and Dosing
The solution was prepared as directed in 2.5. Ninety-six male ICR mice (18–22 g) were randomly and evenly classified into eight

groups (n = 12), including Control (distilled water), Vehicle (corn oil), model (2.5 mg g⁻¹ DEHP daily for 7 days, i.g.), L-carnitine (DEHP for 7 days then 500 mg kg⁻¹ L-carnitine, i.g.), VE (DEHP for 7 days then 100 mg kg⁻¹ VE, i.g.), L-TCE, M-TCE, and H-TCE (DEHP for 7 days then 300, 600, 900 mg kg⁻¹ TCE, i.g.). Treatment was continued for 28 days. The DEHP-induced method has been described in the **Supplementary Material**.

Sample Collection
The animals fasted overnight at the end of the experiment. On the 28th day, the animals were weighed and the anogenital distance (the distance between the penile and anal openings) was measured. Blood samples were centrifuged at 3,500 rpm for 10 min, serum was isolated and stored at −80°C until use. The testes and epididymides samples were removed intact bilaterally, the surrounding fat and connective tissue were stripped and then weighed, and the organ indexes {Organ index = [organ mass (g)/ body mass (g)] * 100%} was calculated. Excising the left testis of each mouse, it was immersed in 4% paraformaldehyde for HE staining and IHC, while the right testis was placed in liquid nitrogen to prepare tissue homogenates for the determination of various parameters.

Testicular Pathological Analysis
Small pieces were removed from the caudal extremity of the testes and fixed in 10% neutral buffered formalin. Proper fixation was followed by dehydration of the specimens in graded ethanol, clearing in xylene, embedding in paraplast, and sectioning at 3–5 μm thickness. The sections were stained using the HE staining method to demonstrate the histological structure of testes in both control and DEHP-induced animals. A Leitz Dialux 20 microscope was adopted to analyze the stained sections. Images were taken using a Canon digital camera (Canon PowerShot A95). Slides were then evaluated for cellular changes in the spermatogenic epithelium.
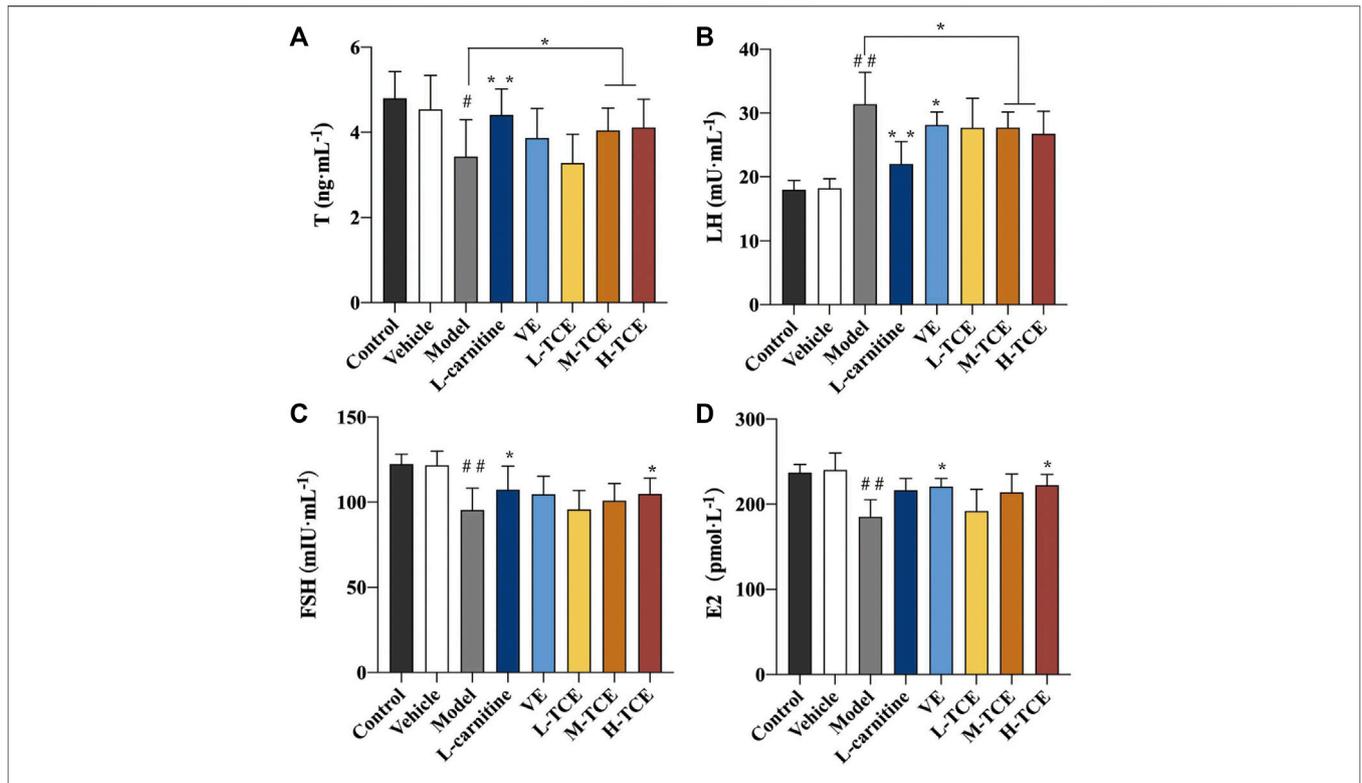
FIGURE 5 | Changes in T, LH, FSH and E2 in the different groups (A). T; (B). LH; (C). FSH; (D). E2; Means ± SD, $n = 12$; $*p < .05$, compared with the model group; $**p < .01$, compared with the model group; $\#\#p < .05$, compared with the control group.
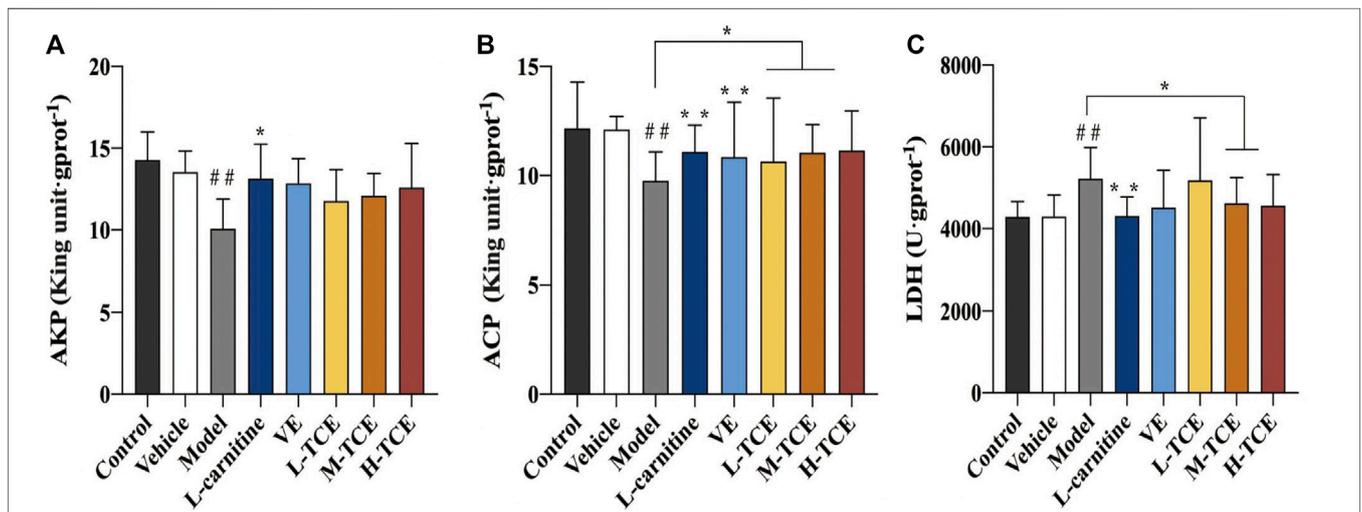
FIGURE 6 | Changes in body AKP, ACP, LDH in the different groups (A). AKP; (B). ACP; (C). LDH; Means ± SD, $n = 12$; $*p < .05$, compared with the model group; $**p < .01$, compared with the model group; $\#\#p < .05$, compared with the control group.

Determination of Sperm Count and Sperm Abnormality Rate

To estimate the sperm count and abnormality rate, the bilateral epididymides was placed in 3 ml of saline pre-warmed to 37°C,

cut up, and placed at 37°C for 1 min before making a sperm suspension.

Determination of sperm count: A drop of sperm suspension was poured into the counting cell (0.1 mm^3) of the hematocrit
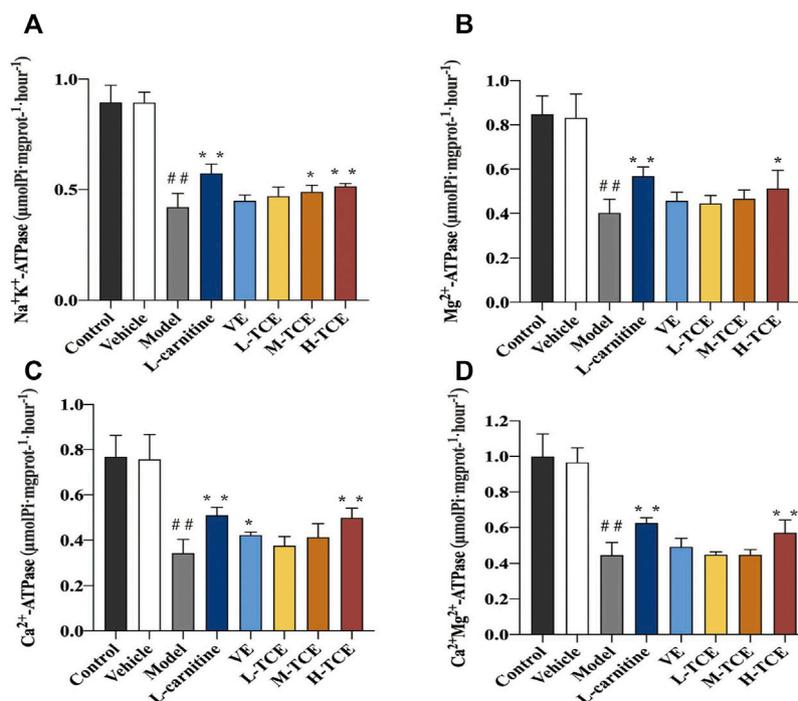
FIGURE 7 | Changes in Na$^+$K$^+$, Mg^{2+}, Ca^{2+}, and Ca^{2+} Mg^{2+}-ATPase in the different groups **(A)**. Na$^+$K$^+$-ATPase; **(B)**. Mg^{2+}-ATPase; **(C)**. Ca^{2+}-ATPase; **(D)**. Ca^{2+} Mg^{2+}-ATPase. Means ± SD, $n = 12$; $*p < .05$, compared with the model group; $**p < .01$, compared with the model group; $##p < .05$, compared with the control group.

plate, the number of sperm in five squares of the counting cell (n) was counted. The total number of sperm in 1 ml (1,000 mm^3) of sperm suspension is 50,000n.

Determination of sperm abnormality rate: The sperm suspension was centrifuged at 1,000 r/min for 5 min, the supernatant was discarded, and the precipitate was mixed with a small amount of the remaining liquid. A suspension drop was placed on a slide and pushed away, dried and fixed in methanol for 5 min, and stained with 2% eosin aqueous solution for 1 h. The morphology of 1,000 sperm was examined to compute the abnormality rate (%).

Determination of Sex Hormones
The concentrations of T, LH, FSH, and E2 in serum were determined as per the instructions of the assay kit. The concentration of the standard served as the horizontal coordinate, whereas the corresponding OD value represented the vertical coordinate to plot a linear regression curve for each hormone. The serum samples were diluted to a certain concentration, and the concentrations were calculated using the standard curve.

Determination of AKP, ACP, and LDH
The assay kit instructions were followed to measure the testicular marker enzymes AKP, ACP, and LDH in testicular tissue homogenates.

Determination of ATPase
The assay kit instructions were followed to measure ATPase activity in testicular tissue homogenates.

Determination of SOD, MDA, GSH-Px, GSH, GR, and CAT
SOD, MDA, and GSH-Px in testicular tissue homogenates were assessed according to the kit instructions.

qRT-PCR Detection of Gene Expression
Testicular tissue samples were collected from the mice as described in 2.6.2, followed by total RNA extraction according to the RNAiso Plus Kit protocol. The total RNA was reverse transcribed into cDNA to estimate its concentration and purity. The synthesized cDNA was subsequently subjected to qRT-PCR analysis. The LightCycler$^®$ 480 Real-Time System was adopted to conduct qPCR and measure the relative expression of the mRNA. The primer sequences for mice *Gapdh* (the housekeeping gene), *Nrf2, HO-1, Keap1, INOS, SOD1, SOD2, SOD3, CAT, PGC1α* (the oxidation-related gene), and *CDC25A, CDC25C, CDK1, Wee1* (the cell cycle control-related gene) and *star, P450scc, CYP11A1, CYP17A1, 3β-HSD, 5α-R, AR, SP1, SF1* (the steroidogenic-related gene) are detailed in **Table 1**.

IHC Studies
The collected testis samples were paraffin sectioned and cut into 5 m thick sections. After blocking endogenous peroxidase, the tissue sections were incubated overnight at 4°C with the primary antibody. The sections were further incubated separately with the secondary antibody for 50 min at room temperature, developed using DAB chromogenic solution, hematoxylin re-stained cell nuclei, and then dehydrated for analysis. The images were

FIGURE 8 | Changes in SOD, MDA, GSH-Px, GSH, GR and CAT in the different groups **(A)**. SOD; **(B)**. MDA; **(C)**. GSH-Px; **(D)**. GSH; **(E)**. GR; **(F)** CAT; Means ± SD, $n = 12$; $*p < .05$, compared with the model group; $**p < .01$, compared with the model group; $##p < .05$, compared with the control group.
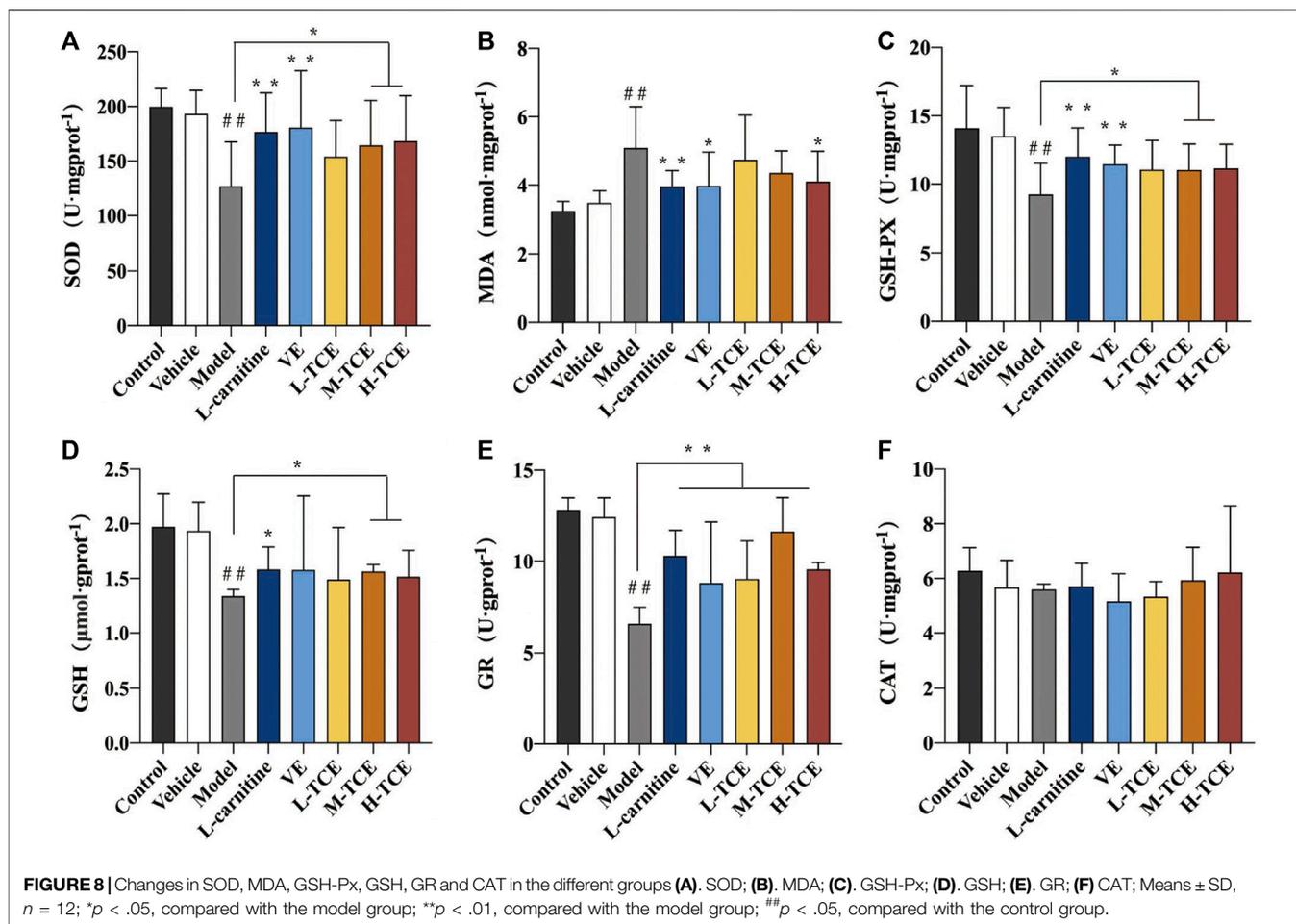
photographed with microscopes and analyzed with Image-pro plus 6.0 (Media Cybernetics, Inc., Rockville, MD, United States). The secondary antibody batch numbers and dilutions are listed in **Table 2**.

Statistical Analysis

All experiments were independently repeated at least three times. Data were expressed as the mean ± SD. One-way analysis of variance (ANOVA) was adopted to scrutinize the quantitative data. $p < .05$ was considered statistically significant ($*p < .05$; $**p < .01$).

RESULTS

Estimation of Total Phenolic Content
Establishment of the Gallic Acid Standard Curve
As illustrated in **Figure 1**, a linear regression equation was obtained: A = 30.116C + 0.0482, $R^2 = 0.999$, with good linearity over the concentration range of (0.001–0.066) $mg \cdot mL^{-1}$ for gallic acid.

Estimation of Total Phenolic Content
Applying the absorbance value to the standard curve equation, a total polyphenol content of (41.07 ± 1.63) mg $GAE \cdot g^{-1}$ was obtained.

Result of Acute Toxicity Test
Pre-Experimental Results
After administration, symptoms such as curling, twitching of the limbs, and cramps were observed in mice within 0.75 h of the maximum dose molding, which lasted for a certain period. The mice manifested signs of idleness, quietness, and reduced activity 1 h post-administration. Some mice also exhibited signs of toxicity, such as diarrhea. The earliest time of death was 0.75 h after administration. The symptoms reduced within 2–3 days among the surviving mice, and they returned to normal in about 4–5 days.

The mortality rate of the 50% alcoholic ethyl acetate fraction was less than 50% within 7 days. The volume and concentration of the drug administered made it difficult to estimate the LD50 value, so a positive MTD was determined based on the pre-test results.

FIGURE 9 | The relative expression levels of nine key oxidation-related genes. **(A)**. *INOS*; **(B)**. *HO-1*; **(C)**. *CAT*; **(D)**. *Nrf2*; **(E)**. *Keap1*; **(F)**. *PGC1α*; **(G)**. *SOD1*; **(H)**. *SOD2*; **(I)**. *SOD3*; Means ± SD; $n = 6$; *$p < .05$, compared with the model group; **$p < .01$, compared with the model group; ##$p < .05$, compared with the control group.
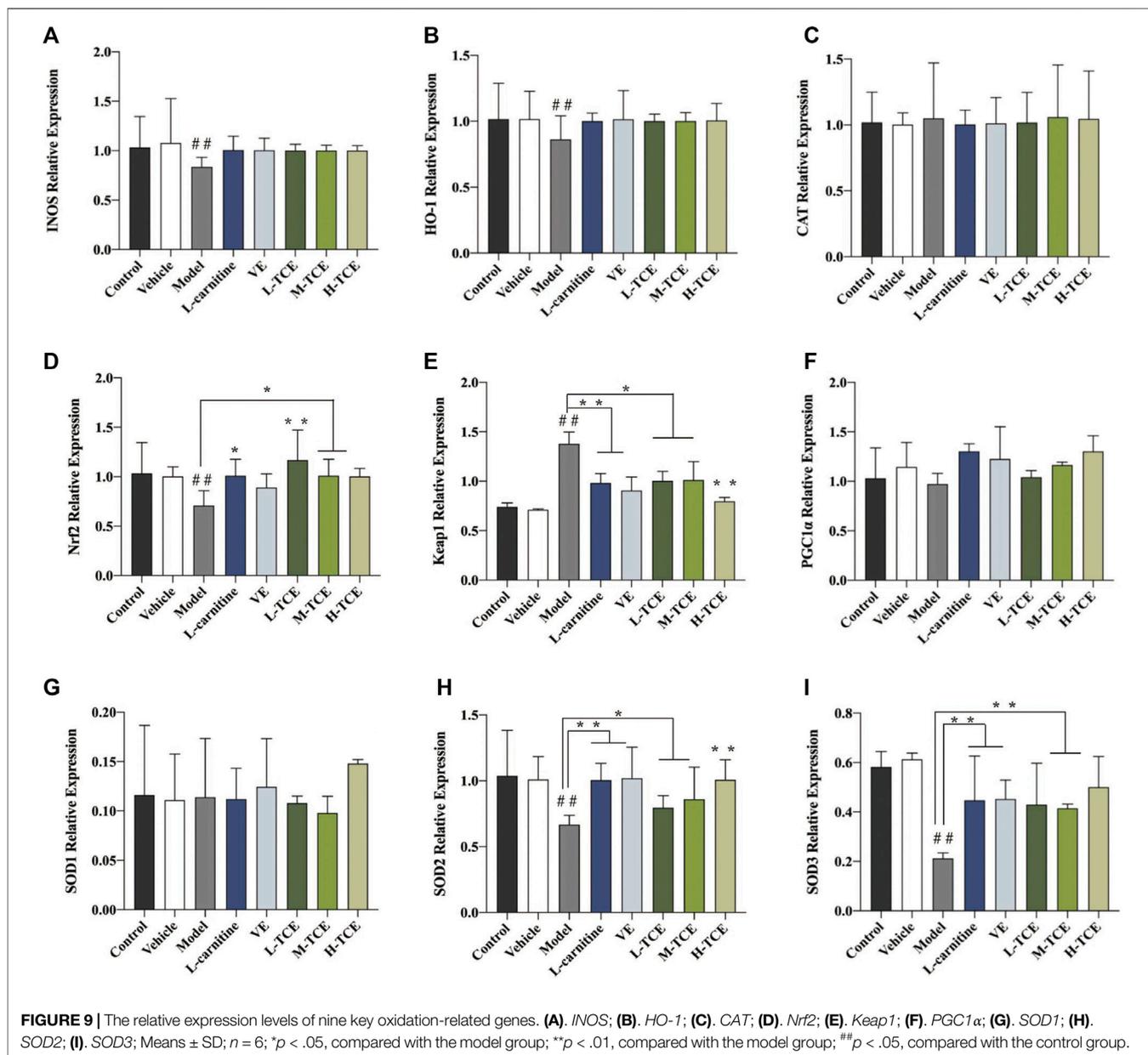
Results of MTD Determination

Following three repeated doses of 900 mg kg^{-1} TCE within 24 h, mice demonstrated signs of toxicity and two mice died within 6 h after the three doses. The approximate MTD of TCE in normal mice was 2.7 g kg^{-1}·d^{-1}.

Results of *in vivo* Efficacy Tests

Results of the Anogenital Distance, Epididymides, and Testis Indexes

As evident from **Figure 2**, a significant decrease in the anogenital distance, epididymides, and testis indexes were noted in the model group compared with the control group ($p < .05$). The indexes in the M-TCE groups were significantly elevated relative to the model group ($p < .05$). The H-TCE groups also demonstrated a significant increase in the epididymides index

($p < .05$). Moreover, a significantly higher anogenital distance was observed in the L-TCE groups than in the model group ($p < .05$).

Testicular Pathological Analysis

The tubule epithelium is made up of spermatogenic and supporting cells, as shown in **Figure 3**. The cells in the control group had normal morphology, were neatly arranged and dense, and contained a lot of sperm in the seminiferous tubules. Compared to the control group, the testicular tissue structure of mice in the model group revealed a small number of atrophied varicoceles, with massive loss of germ cells in the tubules (black arrows), shedding of germ cells in the lumen (red arrows), atrophy of the varicocele and loss of germ cells (yellow arrows), necrosis of germ cells in some of the lumen, fragmentation and lysis of the nucleus, and increased eosinophilia

FIGURE 10 | The relative expression levels of four key cell cycle control-related genes. **(A)**. cdc25A; **(B)**. cdc25C; **(C)**. Wee1; **(D)**. CDK1; Means ± SD; $n = 6$; *$p <$ .05, compared with the model group; **$p <$ .01, compared with the model group; ##$p <$ .05, compared with the control group.
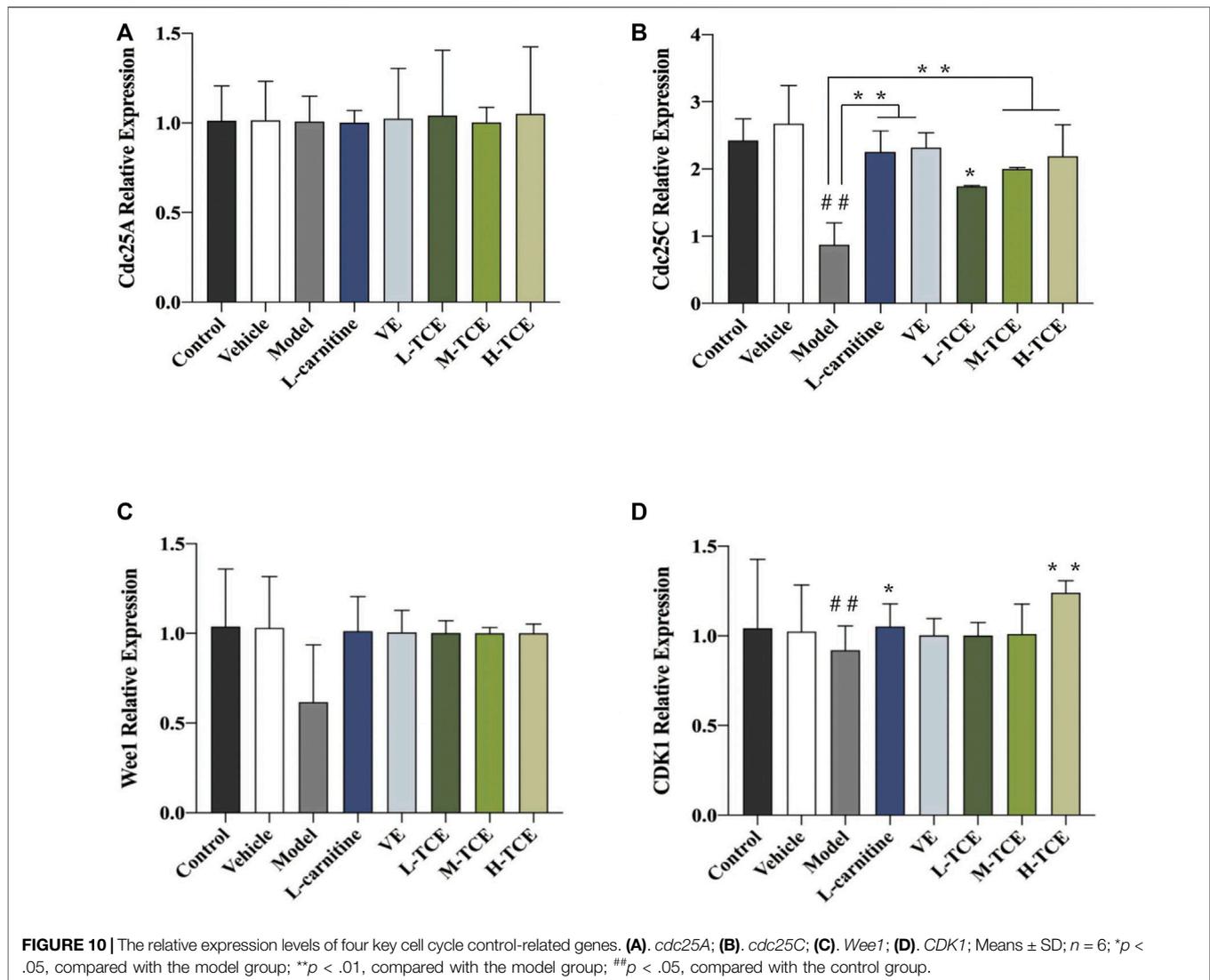
of the cytoplasm (green arrows). Limited improvement in testicular pathology with relief of varicocele dilation, atrophy, and interstitial cell hyperplasia was recorded in the L-TCE, M-TCE, and H-TCE groups, with the best improvement reported by the M-TCE group.

Result of Total Sperm Count and Sperm Abnormality Rate

Significant alteration in the total sperm count and sperm abnormality rate was observed in the model group compared with the control group ($p <$ .05), as confirmed by **Figure 4**. Results substantiated a significant decline in the sperm abnormality rate of the H-TCE group compared with the model group ($p <$ .05).

Result of T, FSH, LH, and E2

Table 3 details the linear equations for the determination of sex hormone content. As indicated by **Figure 5**, induction with DEHP significantly reduced the serum levels of T, FSH and E2, whereas elevated the levels of LH ($p <$ .05). Compared

with the model group, the H-TCE group experienced a significant increase in serum T, FSH and E2 contents, while LH content was decreased ($p <$ .05). The serum level of T and LH were also significantly changed in the M-TCE group relative to that in the model group ($p <$ .05).

Results of AKP, ACP, LDH

The DEHP-induced mice revealed significantly lower levels of AKP and ACP, while higher levels of LDH ($p <$ .05) in the testicular tissue homogenate (**Figure 6**). Compared with the control group, the ACP contents were significantly augmented in the M-TCE and H-TCE groups, whereas the LDH content significantly subsided, and there were significant differences in ACP in the L-TCE group ($p <$ .05). Nonetheless, there was no significant difference in AKP but a dose relationship.

Result of ATPase Activity

As shown in **Figure 7**, the mice induced with DEHP witnessed a significant decline in the testicular tissue homogenate levels for each

FIGURE 11 | The relative expression levels of nine key steroidogenic-related genes. **(A)**. *star*; **(B)**. *P450scc*; **(C)**. *3β-HSD*; **(D)**. *SP1*; **(E)**. *CYP11A1*; **(F)**. *CYP17A1*; **(G)**. *SF1*; **(H)**. *5α-R*; **(I)**. *AR*; Means ± SD; $n = 6$; *$p < .05$, compared with the model group; **$p < .01$, compared with the model group; ##$p < .05$, compared with the control group.
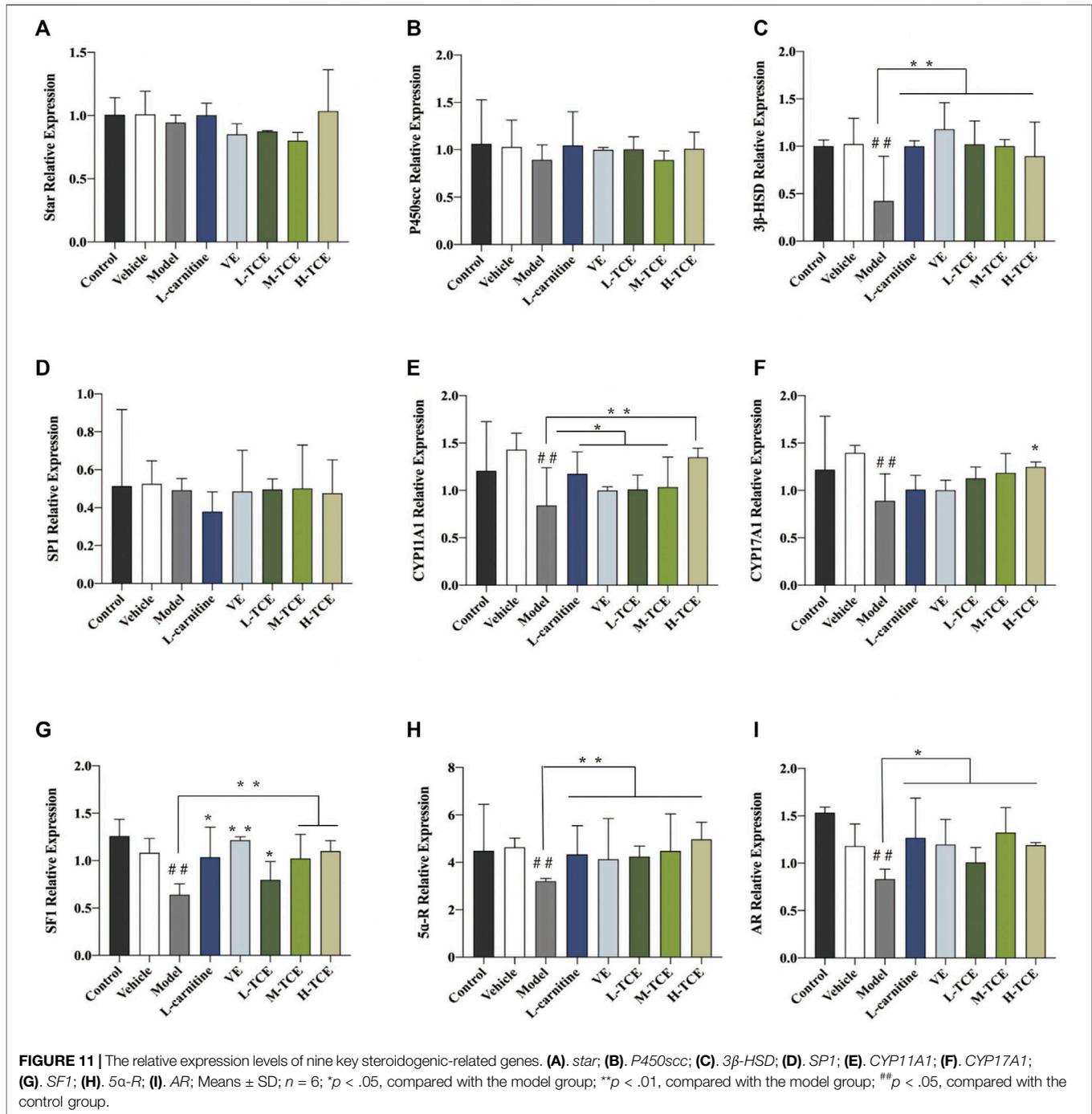
ion channel activity ($p < .05$). In comparison to the control group, the Ca^{2+}Mg^{2+}-ATPase, Mg^{2+}-ATPase and Ca^{2+}-ATPase levels were significantly increased in the H-TCE group, while in the M-TCE and H-TCE groups, Na$^+$K$^+$-ATPase was significantly increased ($p < .05$).

Results of SOD, MDA, GSH-Px, GSH, GR, and CAT

Significant decrease in the activities of SOD, GSH-Px GSH, and the content of GR, and increase in MDA content ($p < .05$) were prominent in the testicular tissue homogenate of the DEHP-induced mice (**Figure 8**). Compared with the control group, the M-TCE and H-TCE groups corroborated significant escalation in the SOD, GSH-Px, and GSH activities, while the MDA content was significantly diminished ($p < .05$) H-TCE group. Moreover, the H-TCE, M-TCE, and L-TCE reflected significant up-regulation in the GR content ($p < .01$), but had no effect in CAT.

FIGURE 12 | IHC analysis of the testis tissues. Immunopositive expression of Nrf2, Keap1, SOD2, SOD3, CDC25C, and CDK1 was observed. Original magnification, ×200.
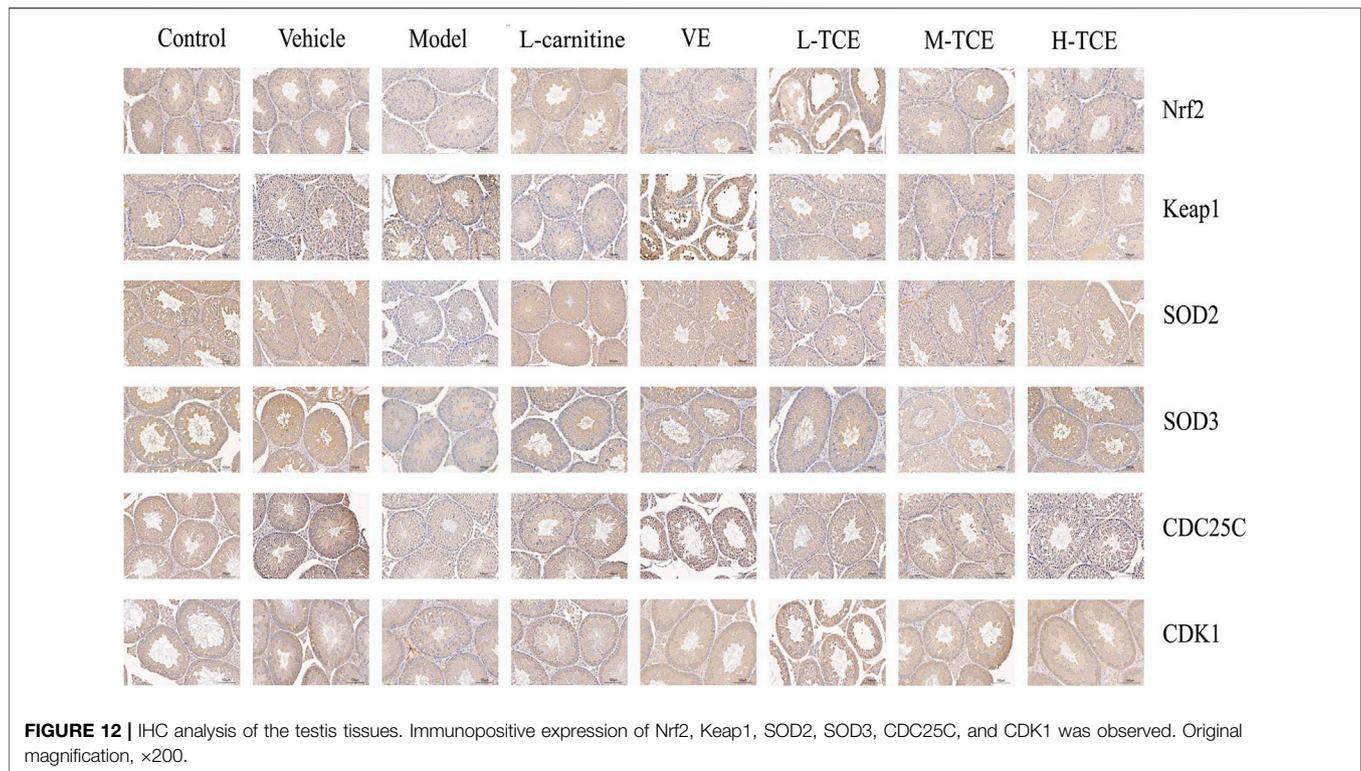
Result of qRT-PCR Detection

The qRT-PCR determined the expression levels of nine key oxidation-related genes, four key cell cycle control-related genes and nine key steroidogenic-related genes (**Figures 9–11**). For the nine key oxidation-related genes, relative to the model group, the H-TCE, M-TCE, and L-TCE could significantly up-regulate the mRNA levels of *Nrf2, SOD2,* and *SOD3,* whereas significantly down-regulate the mRNA levels of *Keap1* ($p < .05$), but did not affect *INOS, HO-1, CAT, PGC1α,* and *SOD1*. Compared with the model group, for the four key testicular cell cycle control-related genes, the H-TCE, M-TCE, and L-TCE reflected significant up-regulation in the mRNA levels of *CDC25C,* and *CDK1* ($p < .05$); but had no effect on *CDC25A, Wee1*. For the nine key steroidogenic-related genes, compared with the model group, the H-TCE, M-TCE, and L-TCE could significantly up-regulate the mRNA levels of *CYP11A1,3β-HSD, 5α-R, AR,* the M-TCE, and H-TCE reflected significant up-regulation in the mRNA levels of *SF1,* and significant up-regulation in the mRNA levels of *CYP17A1* in the H-TCE. Nonetheless, there was no significant difference in *SP1, P450scc* and *Star*.

IHC Studies

A brownish-yellow area represented a positive result, indicating antigen-antibody binding on germ cells. The mean density is computed as the ratio of the cumulative optical density value (IOD) to the pixel area of the tissue (AREA) for each positive photograph, and the immunohistochemical results can be interpreted by analyzing mean density. The lower mean density of Nrf2, SOD2, SOD3, CDC25C, and CDK1 proteins

in the DEHP group signified weaker immunopositive staining and lower protein expression for each protein following DEHP induction. The higher mean density of Keap1 proteins in the DEHP group signified higher protein expression following DEHP induction ($p < .01$). However, in the TCE group, the testicular tissue revealed a trend of significantly enhanced positive responses to Nrf2, SOD2, SOD3, CDC25C, and CDK1 proteins with significantly higher protein expression and a trend of significantly reduced positive responses to Keap1 proteins with significantly lower protein expression (**Figures 12, 13**).

DISCUSSION

TCE-Mediated Alleviation of the Oxidative Stress Caused by DEHP

The findings of this study suggested that DEHP considerably increased MDA content in testicular serum, while GSH, GSH-Px, SOD vitality, and GR content were significantly reduced, indicating that DEHP staining in testicular tissue failed to remove reactive oxygen free radicals effectively. This resulted in excessive accumulation of oxygen free radicals, which, in turn, triggered lipid peroxidation, ultimately leading to cell damage. Significantly affecting the testicular tissue oxidation and antioxidant enzyme content, H-TCE enabled the repair of the DEHP-induced oxidative damage of testicular tissue. The effect of TCE in modifying the activity of SOD and other oxidation indicators encouraged us to study the activity of related genes by qRT-PCR. Results emphasized TCE-mediated significant
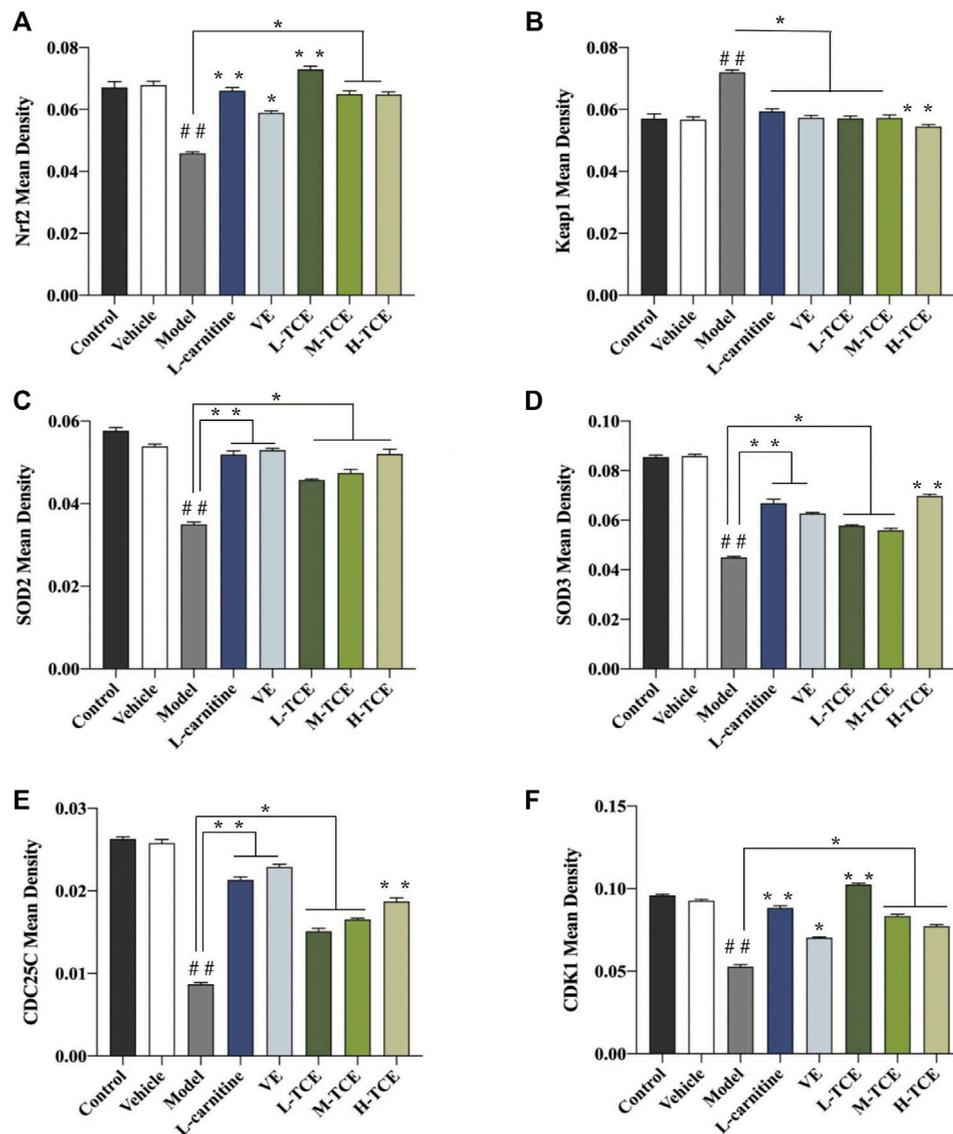
FIGURE 13 | The mean density of six antibodies. **(A)**. Nrf2; **(B)**. Keap1; **(C)**. SOD2; **(D)**. SOD3; **(E)**. CDC25C; **(F)**. CDK1; Means ± SD; $n = 6$; $*p < .05$, compared with the model group; $**p < .01$, compared with the model group; $^{\#\#}p < .05$, compared with the control group.

increase in the expression levels of *Nrf2, SOD2,* and *SOD3, a* significant decrease in the expression levels of *Keap1.* IHC further substantiated this finding at the protein level. Keap1-Nrf2 pathway plays a crucial role in antioxidant activity. In the resting state, *Nrf2* binds to Keap1 in the cytoplasm and is inactive. When the body is in a state of oxidative stress, *Nrf2* is uncoupled with *Keap1* and transferred into the nucleus, where it binds with antioxidant reaction elements (ARE) to activate the expression of downstream antioxidant protein genes to reduce oxidative damage (Papaiahgari et al., 2007; Ma, 2013). TCE may stimulate oxidative degradation of *Keap1* in testicular tissue cytoplasm, promote dissociation of Keap1-Nrf2 coupling, increase nuclear translocation and expression of *Nrf2*, and then activate transcription of antioxidant enzymes such as

SOD, GSH, and GSH-Px downstream to enhance antioxidant damage ability and resist testicular injury (Uruno and Motohashi, 2011). The increase of SOD enzyme activity can reduce the ROS generation and regulate the level of O^{2-}; thus, minimizing the detrimental effect of oxidative stress and maintaining normal tissue function (Schram et al., 2019). TCE's better anti-oxidative activity of the reproductive system may be realized by up-regulating SOD family expression and Keap1-Nrf2 signaling pathway.

The phenolic compounds may be the pharmacologically active ingredients responsible for the antioxidant activity of TCE. Phenolic compounds are a special type of secondary metabolite, with phenolic radicals having a lower electron reduction potential than that of oxygen radicals (Bors et al.,

1990; Grace, 2005) and the capacity to quench radicals by forming resonance-stabilized phenoxy groups (Rice-Evans et al., 1996; Bors and Michel, 2002). Thus, by scavenging the intermediates of reactive oxygen species, these phenolic compounds restrict the promotion of further oxidation reactions (Grace, 2005). By maintaining the homeostasis between oxidants and antioxidants, they play a vital role in combating oxidative stress in humans (Manach et al., 2005; Dudonné et al., 2009).

TCE Improved the Energy Metabolism

ATPase is a widely present key enzyme in testicular energy metabolism, affecting energy production, transfer, and utilization. It also regulates normal membrane potential changes in cell membranes, thereby maintaining the stability of the internal environment. The reductions of ATPase and reduced ATP production exert a crucial impact on tissue damage (Pivovarova et al., 1992). This investigation revealed a significant reduction in ATPase activity following DEHP induction, and this indicated that DEHP-induced inhibition of ATPase activity affects the testicular spermatogenic cells to carry out energy conversion. This, in turn, impaired the development of the testis and epididymides, causing damage to the spermatogenic cells and affecting the spermatogenic process. Alteration in testicular and epididymides organ indexes and sperm-related parameters further substantiated these findings. In this study, DEHP-induced inhibition of gonadal organ development, a decline in organ coefficients of testes and epididymides, and an increase in sperm aberration rate all confirmed the abnormal energy metabolic process of the reproductive system. H-TCE was able to restore enzyme activities and organ indices, and sperm-related parameters to some extent, indicating that TCE reinstated the energy metabolic process of the reproductive system to a certain degree.

TCE Improved the Testicular Function

Moreover, changes in sex hormones and testicular marker enzymes reflect modification in testicular function. The major physiological function of T, mostly synthesized and secreted by testicular mesenchymal cells, is to maintain normal spermatogenesis and promote the development and maturation of the testicular parenchymal organs (Han et al., 2021). The hypothalamic-pituitary-testicular axis (HPTA) is primarily engaged in regulating the synthesis and secretion of testosterone, which may also be regulated by feedback from LH and FSH (Recabarren et al., 2013; Ha et al., 2016). The entry of the capital products of T into the reproductive system following DEHP stimulation may damage mesenchymal cells through oxidative damage and other pathways, resulting in a decrease in T levels. It may also produce large amounts of estrogen, interfering with the normal function of HPTA and affecting the secretion of LH and thus testosterone. This diminishes the serum testosterone levels in mice, decreases its binding to androgen receptors in spermatogenic cells, thereby inhibiting spermatogenesis.

AKP activity is linked to the division of testicular spermatogenic cells at all stages, as well as with the energy transport of glucose. ACP is most abundant in the cytoplasm

of testicular supporting cells and is involved in spermatogenic cell synthesis and phagocytosis. It plays a vital role in protein synthesis and supports normal physiological metabolism and function. Changes in its activity are directly related to the degeneration of the germinal epithelium (Zheng et al., 2010). LDH is a testis-specific marker enzyme, closely linked with the germinal process, and changes in its activity can respond characteristically to the lethal effects of chemical toxicants on the testis (Hodgen and Sherins, 1973; Yang et al., 2010). Interfering with glycolysis and aerobic respiration in germinal cells, DEHP can lead to an inadequate supply of energy, affecting spermatogenesis and maturation. H-TCE significantly altered ACP and LDH, reversing the effects triggered by DEHP and facilitating energy transfer to testicular tissue.

Estimation of the cell cycle control-related genes claimed a significant decrease in CDK1 and CDC25C levels following DEHP induction. CDK1 is a nonredundant cyclin-dependent kinase with an essential role in mitosis (Vassilev et al., 2006). Studies have established a correlation of the activation of this kinase with cell death of postmitotic neurons in brain development and disease (Yuan et al., 2008). CDC25C, a dual-specificity protein phosphatase, monitors the entry of cells into mitosis by dephosphorylating the protein kinase Cdc2 (Peng et al., 1997). Phosphorylation on serine 216 is observed throughout interphase but not during mitosis (Peng et al., 1998). The present study documented that exposure to DEHP impaired the CDC25C-CDK1 interaction during mitosis. This decelerates the metabolism of spermatogenic cells, curtailing sperm growth and maturation. The M-TCE and H-TCE facilitated a significant upsurge in the expression of CDK1, CDC25C, proposing the role of TCE in promoting CDC25C-CDK1 interaction, which in turn stimulates spermatogenic cell proliferation, testicular development, and sperm development and maturation.

Testosterone in the Leydig cells of synthetic process for combining with the status of cholesterol in the blood after receptor transport into the Leydig cell cytoplasm, with the help of STAR, and so on factor into the mitochondrial membrane, on P450SCC, mitochondrial membrane cholesterol cracking can become pregnenolone, is the first step on the testosterone generated in this reaction, It is also the rate-limiting step of testosterone production (Agarwal and Auchus, 2005). After the synthesis of pregnenolone, it is transferred to the smooth endoplasmic reticulum by diffusion, where it is rapidly digested into progesterone by 3β-HSD. 3β-HSD is one of the key enzymes of the steroid hormone synthesis pathway and is expressed in testicular interstitial cells. It is recognized as a marker of testicular interstitial cells. Its activity is also an important indicator to measure the ability of interstitial cells to synthesize testosterone, which is the basic step of all bioactive steroid hormone synthesis (Trant et al., 1990; Sawicki et al., 1999; Zylka et al., 2008). CYP11A1 and CYP17A1 are important enzymes in the transformation of pregnenolone to androgen (Sushko et al., 2012; Bloem et al., 2013). SF1 affects testosterone androgen synthesis by interfering with the signal transduction pathway of steroid hormone synthesis and interfering with the expression of genes and proteins related to cholesterol transport or androgen synthesis. 5α-R is a specific enzyme that catalyzes the transformation of testosterone into

dihydrotestosterone (DHT). The high expression of DHT can promote the development of organs such as testis and epididymides, which is consistent with the results of organ coefficient measurement. Its activity also affects the development and maturation of sperm. AR is the only receptor for androgen binding, and its higher expression level indicates that the number of androgen binding receptors is increased to promote androgen activity (Poletti and Martini, 1999; Wang et al., 2019). Compared with the control group, the relative expression levels of *3β-HSD, CYP11A1, CYP17A1, AR,* and *5α -R, SP1* were decreased. Compared with the model group, 900 mg kg^{-1} generally increased the relative expression levels of the above genes.

CONCLUSION

Our results suggest that M-TCE and H-TCE was able to alleviate DEHP-induced reproductive system damage in male mice by improving testicular histopathology, repairing testicular function, and reducing oxidative stress damage. The differences in indicators among the groups showed that TCE significantly improved the anogenital distance and the organ indexes of the epididymides and testes. It also significantly reduced the extent of varicocele and interstitial cell lesions compared to the model group. H-TCE reduced the sperm abnormality rate, increased the levels of sex hormones, Na$^+$K$^+$ and Mg^{2+}, Ca^{2+}-ATPase enzyme activity, antioxidant enzyme vitality, along a significant decrease in LH and MDA contents. The levels of testicular marker enzymes ACP and LDH were significantly augmented by both M-TCE and H-TCE. qRT-PCR and IHC results indicated that the mechanistic approach behind the protective effects of TCE might be attributed to the oxidation-related Keap1-Nrf2 pathway, SODs enzyme, the cell cycle control-related CDC25C-CDK1 pathway, and the steroidogenic-related pathway. Thus, in summary, our results confirmed the beneficial effects of *Trichilia catigua* on male mice reproduction. The mechanisms of the beneficial effects are complex and ambiguous but may include the modulation of antioxidant, energy metabolism, and testicular function.

In this study, the mechanism of TCE against oxidative damage in the reproductive system was preliminarily discussed. However, as the mechanism of testicular tissue function is complex and changeable, this mechanism is only one of the possible ways. Subsequent studies can explore the inhibition of mitochondrial damage and apoptosis to study the mechanism of TCE in a more systematic and in-depth way.

DATA AVAILABILITY STATEMENT

The original contributions presented in the study are included in the article/**Supplementary Material**, further inquiries can be directed to the corresponding authors.

ETHICS STATEMENT

The animal study was reviewed and approved by the research animal ethics committee of the Institute of Medicinal Plant Development affiliated with the Chinese Academy of Medical Sciences (Beijing, China).

AUTHOR CONTRIBUTIONS

XC, JL, and XYC: design experiments scheme. XYC and MH: data processing and analyzing. XYC, MD, and XM: mice experiments and measurement of biochemical indicators. XC and JL: redaction and supervisor of the work. All authors agree to be accountable for the content of the work.

FUNDING

SUPPLEMENTARY MATERIAL

The Supplementary Material for this article can be found online at: https://www.frontiersin.org/articles/10.3389/fphar.2022.832789/full#supplementary-material

REFERENCES

Abd-Ellah, M. F., Aly, H. A., Mokhlis, H. A., and Abdel-Aziz, A. H. (2016). Quercetin Attenuates Di-(2-ethylhexyl) Phthalate-Induced Testicular Toxicity in Adult Rats. *Hum. Exp. Toxicol.* 35 (3), 232–243. doi:10.1177/0960327115580602

Agarwal, A. K., and Auchus, R. J. (2005). Minireview: Cellular Redox State Regulates Hydroxysteroid Dehydrogenase Activity and Intracellular Hormone Potency. *Endocrinology* 146 (6), 2531–2538. doi:10.1210/en.2005-0061

Andrade, A. J., Grande, S. W., Talsness, C. E., Grote, K., Golombiewski, A., Sterner-Kock, A., et al. (2006). A Dose-Response Study Following In Utero and Lactational Exposure to Di-(2-ethylhexyl) Phthalate (DEHP): Effects on Androgenic Status, Developmental Landmarks and Testicular Histology in Male Offspring Rats. *Toxicology* 225 (1), 64–74. doi:10.1016/j.tox.2006.05.007

Antunes, E., Gordo, W. M., de Oliveira, J. F., Teixeira, C. E., Hyslop, S., and De Nucci, G. (2001). The Relaxation of Isolated Rabbit Corpus Cavernosum by the Herbal Medicine Catuama and its Constituents. *Phytother Res.* 15 (5), 416–421. doi:10.1002/ptr.861

Barakat, R., Lin, P. P., Rattan, S., Brehm, E., Canisso, I. F., Abosalum, M. E., et al. (2017). Prenatal Exposure to DEHP Induces Premature Reproductive Senescence in Male Mice. *Toxicol. Sci.* 156 (1), 96–108. doi:10.1093/toxsci/kfw248

Barakat, R., Seymore, T., Lin, P. P., Park, C. J., and Ko, C. J. (2019). Prenatal Exposure to an Environmentally Relevant Phthalate Mixture Disrupts Testicular Steroidogenesis in Adult Male Mice. *Environ. Res.* 172, 194–201. doi:10.1016/j.envres.2019.02.017

Barbosa, N. R., Fischmann, L., Talib, L. L., and Gattaz, W. F. (2004). Inhibition of Platelet Phospholipase A2 Activity by Catuaba Extract Suggests Antiinflammatory Properties. *Phytother Res.* 18 (11), 942–944. doi:10.1002/ptr.1579

Bernardo, J., Ferreres, F., Gil-Izquierdo, Á., Videira, R. A., Valentão, P., Veiga, F., et al. (2018). *In Vitro* multimodal-effect of Trichilia Catigua A. Juss. (Meliaceae) Bark Aqueous Extract in CNS Targets. *J. Ethnopharmacol* 211, 247–255. doi:10.1016/j.jep.2017.09.039

Bloem, L. M., Storbeck, K. H., Schloms, L., and Swart, A. C. (2013). 11β-hydroxyandrostenedione Returns to the Steroid arena: Biosynthesis, Metabolism and Function. *Molecules* 18 (11), 13228–13244. doi:10.3390/molecules181113228

Bors, W., Heller, W., Michel, C., and Saran, M. (1990). Flavonoids as Antioxidants: Determination of Radical-Scavenging Efficiencies. *Methods Enzymol.* 186, 343–355. doi:10.1016/0076-6879(90)86128-i

Bors, W., and Michel, C. (2002). Chemistry of the Antioxidant Effect of Polyphenols. *Ann. N. Y Acad. Sci.* 957, 57–69. doi:10.1111/j.1749-6632.2002.tb02905.x

Damstra, T., Barlow, S., Bergman, A., Kavlock, R., and Van Der Kraak, G. (2002). *World Health Organization: Global Assessment of the State of the Science of Endocrine Disruptors.* Geneva: WHO, 180.

do Nascimento Bonato Panizzon, C. P., de Miranda Neto, M. H., Ramalho, F. V., Longhini, R., de Mello, J. C. P., and Zanoni, J. N. (2019). Ethyl Acetate Fraction from Trichilia Catigua Confers Partial Neuroprotection in Components of the Enteric Innervation of the Jejunum in Diabetic Rats. *Cell Physiol Biochem* 53 (1), 76–86. doi:10.33594/000000122

Dudonné, S., Vitrac, X., Coutière, P., Woillez, M., and Mérillon, J.-M. (2009). Comparative Study of Antioxidant Properties and Total Phenolic Content of 30 Plant Extracts of Industrial Interest Using DPPH, ABTS, FRAP, SOD, and ORAC Assays. *J. Agric. Food Chem.* 57 (5), 1768–1774. doi:10.1021/jf803011r

Farombi, E. O., Abarikwu, S. O., Adedara, I. A., and Oyeyemi, M. O. (2007). Curcumin and Kolaviron Ameliorate Di-n-butylphthalate-induced Testicular Damage in Rats. *Basic Clin. Pharmacol. Toxicol.* 100 (1), 43–48. doi:10.1111/j.1742-7843.2007.00005.x

Grace, S. C. (2005). *Antioxidants and Reactive Oxygen Species in Plants (Smirnoff/Antioxidants) ‖ Phenolics as Antioxidants.* Oxford, UK: Blackwell Publishing.

Ha, M., Guan, X., Wei, L., Li, P., Yang, M., and Liu, C. (2016). Di-(2-ethylhexyl) Phthalate Inhibits Testosterone Level through Disturbed Hypothalamic-Pituitary-Testis axis and ERK-Mediated 5α-Reductase 2. *Sci. Total Environ.* 563-564, 566–575. doi:10.1016/j.scitotenv.2016.04.145

Han, Y., Si, W., Han, Y., Na, R., Zeng, Y., E, G., et al. (2021). Immunization with Oral KISS1 DNA Vaccine Inhibits Testicular Leydig Cell Proliferation Mainly via the Hypothalamic-Pituitary-Testicular axis and Apoptosis-Related Genes in Goats. *Anim. Biotechnol.* 32 (3), 395–399. doi:10.1080/10495398.2019.1697701

Hodgen, G. D., and Sherins, R. J. (1973). Enzymes as Markers of Testicular Growth and Development in the Rat. *Endocrinology* 93 (4), 985–989. doi:10.1210/endo-93-4-985

Kamdem, J. P., Waczuk, E. P., Kade, I. J., Wagner, C., Boligon, A. A., Athayde, M. L., et al. (2012). Catuaba (Trichilia Catigua) Prevents against Oxidative Damage Induced by *In Vitro* Ischemia-Reperfusion in Rat Hippocampal Slices. *Neurochem. Res.* 37 (12), 2826–2835. doi:10.1007/s11064-012-0876-0

Longhini, R., Lonni, A. A. S. G., Sereia, A. L., Krzyzaniak, L. M., Lopes, G. C., and Mello, J. C. P. de. (2017). Trichilia Catigua : Therapeutic and Cosmetic Values. *Revista Brasileira De Farmacognosia* 27 (2), 254–271. doi:10.1016/j.bjp.2016.10.005

Lyche, J. L., Gutleb, A. C., Bergman, A., Eriksen, G. S., Murk, A. J., Ropstad, E., et al. (2009). Reproductive and Developmental Toxicity of Phthalates. *J. Toxicol. Environ. Health B Crit. Rev.* 12 (4), 225–249. doi:10.1080/10937400903094091

Ma, Q. (2013). Role of Nrf2 in Oxidative Stress and Toxicity. *Annu. Rev. Pharmacol. Toxicol.* 53, 401–426. doi:10.1146/annurev-pharmtox-011112-140320

Manach, C., Williamson, G., Morand, C., Scalbert, A., and Rémésy, C. (2005). Bioavailability and Bioefficacy of Polyphenols in Humans. I. Review of 97 Bioavailability Studies. *Am. J. Clin. Nutr.* 81 (1 Suppl. l), 230s–242s. doi:10.1093/ajcn/81.1.230S

Merzenich, H., Zeeb, H., and Blettner, M. (2010). Decreasing Sperm Quality: a Global Problem. *BMC Public Health* 10, 24. doi:10.1186/1471-2458-10-24

Muczynski, V., Lecureuil, C., Messiaen, S., Guerquin, M. J., N'Tumba-Byn, T., Moison, D., et al. (2012). Cellular and Molecular Effect of MEHP Involving LXRα in Human Fetal Testis and Ovary. *PLoS One* 7 (10), e48266. doi:10.1371/journal.pone.0048266

Oliveira, C. H., Moraes, M. E., Moraes, M. O., Bezerra, F. A., Abib, E., and De Nucci, G. (2005). Clinical Toxicology Study of an Herbal Medicinal Extract of Paullinia Cupana, Trichilia Catigua, Ptychopetalum Olacoides and Zingiber Officinale (Catuama) in Healthy Volunteers. *Phytother Res.* 19 (1), 54–57. doi:10.1002/ptr.1484

Papaiahgari, S., Yerrapureddy, A., Hassoun, P. M., Garcia, J. G., Birukov, K. G., and Reddy, S. P. (2007). EGFR-activated Signaling and Actin Remodeling Regulate Cyclic Stretch-Induced NRF2-ARE Activation. *Am. J. Respir. Cel Mol Biol* 36 (3), 304–312. doi:10.1165/rcmb.2006-0131OC

Peng, C. Y., Graves, P. R., Ogg, S., Thoma, R. S., Byrnes, M. J., 3rd, Wu, Z., et al. (1998). C-TAK1 Protein Kinase Phosphorylates Human Cdc25C on Serine 216 and Promotes 14-3-3 Protein Binding. *Cell Growth Differ* 9 (3), 197–208.

Peng, C. Y., Graves, P. R., Thoma, R. S., Wu, Z., Shaw, A. S., and Piwnica-Worms, H. (1997). Mitotic and G2 Checkpoint Control: Regulation of 14-3-3 Protein Binding by Phosphorylation of Cdc25C on Serine-216. *Science* 277 (5331), 1501–1505. doi:10.1126/science.277.5331.1501

Pivovarova, N. B., Lagerspetz, K., and Skulskii, I. A. (1992). Effect of Cadmium on Ciliary and ATPase Activity in the Gills of Freshwater Mussel Anodonta Cygnea. *Comp. Biochem. Physiol. C Comp. Pharmacol.* 103 (1), 27–30. doi:10.1016/0742-8413(92)90223-t

Pizzolatti, M. G., Venson, A. F., Smânia, A., Jr., Smânia Ede, F., and Braz-Filho, R. (2002). Two Epimeric Flavalignans from Trichilia Catigua (Meliaceae) with Antimicrobial Activity. *Z. Naturforsch C J. Biosci.* 57 (5-6), 483–488. doi:10.1515/znc-2002-5-614

Poletti, A., and Martini, L. (1999). Androgen-activating Enzymes in the central Nervous System. *J. Steroid Biochem. Mol. Biol.* 69 (1-6), 117–122. doi:10.1016/s0960-0760(98)00150-2

Recabarren, M. P., Rojas-Garcia, P. P., Einspanier, R., Padmanabhan, V., Sir-Petermann, T., and Recabarren, S. E. (2013). Pituitary and Testis Responsiveness of Young Male Sheep Exposed to Testosterone Excess during Fetal Development. *Reproduction* 145 (6), 567–576. doi:10.1530/rep-13-0006

Rice-Evans, C. A., Miller, N. J., and Paganga, G. (1996). Structure-antioxidant Activity Relationships of Flavonoids and Phenolic Acids. *Free Radic. Biol. Med.* 20 (7), 933–956. doi:10.1016/0891-5849(95)02227-9

Saunders, P. T., Majdic, G., Parte, P., Millar, M. R., Fisher, J. S., Turner, K. J., et al. (1997). Fetal and Perinatal Influence of Xenoestrogens on Testis Gene Expression. *Adv. Exp. Med. Biol.* 424, 99–110. doi:10.1007/978-1-4615-5913-9_19

Sawicki, M. W., Erman, M., Puranen, T., Vihko, P., and Ghosh, D. (1999). Structure of the Ternary Complex of Human 17beta-Hydroxysteroid Dehydrogenase Type 1 with 3-Hydroxyestra-1,3,5,7-Tetraen-17-One (Equilin) and NADP+. *Proc. Natl. Acad. Sci. U S A.* 96 (3), 840–845. doi:10.1073/pnas.96.3.840

Schram, S., Chuang, D., Schmidt, G., Piponov, H., Helder, C., Kerns, J., et al. (2019). Mutant SOD1 Prevents normal Functional Recovery through Enhanced Glial Activation and Loss of Motor Neuron Innervation after Peripheral Nerve Injury. *Neurobiol. Dis.* 124, 469–478. doi:10.1016/j.nbd.2018.12.020

Silva, A. J. d. (2004). Estudo botanico e chimico da catuaba (Erythroxylaceae Catuaba Do Norte). *Revista Brasileira De Farmacognosia* 14 (2), 145–151. doi:10.1590/s0102-695x2004000100009

Slinkard, K., and Singleton, V. L. (1977). Total Phenol Analysis: Automation and Comparison with Manual Methods. *Am. J. Enology Viticulture* 28 (1), 49–55.

Street, M. E., Angelini, S., Bernasconi, S., Burgio, E., Cassio, A., Catellani, C., et al. (2018). Current Knowledge on Endocrine Disrupting Chemicals (EDCs) from Animal Biology to Humans, from Pregnancy to Adulthood: Highlights from a National Italian Meeting. *Int. J. Mol. Sci.* 19 (6). doi:10.3390/ijms19061647

Sushko, T. A., Gilep, A. A., and Usanov, S. A. (2012). Mechanism of Intermolecular Interactions of Microsomal Cytochrome P450s CYP17 and CYP21 Involved in Steroid Hormone Biosynthesis. *Biochemistry (Mosc)* 77 (6), 585–592. doi:10.1134/s0006297912060041

Tang, W., Hioki, H., Harada, K., Kubo, M., and Fukuyama, Y. (2007). Antioxidant Phenylpropanoid-Substituted Epicatechins from Trichilia Catigua. *J. Nat. Prod.* 70 (12), 2010–2013. doi:10.1021/np0703895

Trant, J. M., Lorence, M. C., Johnson, E. F., Shackleton, C. H., Mason, J. I., and Estabrook, R. W. (1990). Characterization of the Steroid-Metabolizing Capacity of the Hepatic Cytochrome P450IIC5 Expressed in COS-1 Cells: 3 Beta-Hydroxysteroid Dehydrogenase/delta 5----4 Isomerase Type Activity. *Proc. Natl. Acad. Sci. U S A.* 87 (24), 9756–9760. doi:10.1073/pnas.87.24.9756

Uruno, A., and Motohashi, H. (2011). The Keap1-Nrf2 System as an *In Vivo* Sensor for Electrophiles. *Nitric Oxide* 25 (2), 153–160. doi:10.1016/j.niox.2011.02.007

Vassilev, L. T., Tovar, C., Chen, S., Knezevic, D., Zhao, X., Sun, H., et al. (2006). Selective Small-Molecule Inhibitor Reveals Critical Mitotic Functions of Human CDK1. *Proc. Natl. Acad. Sci. U S A.* 103 (28), 10660–10665. doi:10.1073/pnas.0600447103

Wang, Y., Li, H., Zhu, Q., Li, X., Lin, Z., and Ge, R. S. (2019). The Cross Talk of Adrenal and Leydig Cell Steroids in Leydig Cells. *J. Steroid Biochem. Mol. Biol.* 192, 105386. doi:10.1016/j.jsbmb.2019.105386

Yang, J., Wu, G., Feng, Y., Lv, Q., Lin, S., and Hu, J. (2010). Effects of Taurine on Male Reproduction in Rats of Different Ages. *J. Biomed. Sci.* 17 (Suppl. 1), S9. doi:10.1186/1423-0127-17-s1-s9

Yeung, B. H., Wan, H. T., Law, A. Y., and Wong, C. K. (2011). Endocrine Disrupting Chemicals: Multiple Effects on Testicular Signaling and Spermatogenesis. *Spermatogenesis* 1 (3), 231–239. doi:10.4161/spmg.1.3.18019

Yuan, Z., Becker, E. B., Merlo, P., Yamada, T., DiBacco, S., Konishi, Y., et al. (2008). Activation of FOXO1 by Cdk1 in Cycling Cells and Postmitotic Neurons. *Science* 319 (5870), 1665–1668. doi:10.1126/science.1152337

Zheng, S. J., Tian, H. J., Cao, J., and Gao, Y. Q. (2010). Exposure to di(n-butyl) phthalate and benzo(a)pyrene alters IL-1β secretion and subset expression of testicular macrophages, resulting in decreased testosterone production in rats. *Toxicol. Appl. Pharmacol.* 248 (1), 28–37. doi:10.1016/j.taap.2010.07.008

Zylka, M. J., Sowa, N. A., Taylor-Blake, B., Twomey, M. A., Herrala, A., Voikar, V., et al. (2008). Prostatic Acid Phosphatase Is an Ectonucleotidase and Suppresses Pain by Generating Adenosine. *Neuron* 60 (1), 111–122. doi:10.1016/j.neuron.2008.08.024